Available online at www.sciencedirect.com
ScienceDirect
Polyhedron 26 (2007) 749–756
POLYHEDRON
www.elsevier.com/locate/poly

Synthesis, spectral characterization and structural investigation on some 4-aminoantipyrine containing Schiff base Cu(II) complexes and their molecular association

P. Mosae Selvakumar, E. Suresh *, P.S. Subramanian *

Analytical Science Division, Central Salt and Marine Chemicals Research Institute (CSIR), Gijubhai Badhegha Marg, Bhavnagar, Gujarat 364 002, India

Received 1 August 2006; accepted 4 September 2006
Available online 22 September 2006

Abstract

Compounds $[Cu(L_1)_2]$ (**1**) and $[Cu(L_2)_2]$ (**2**), where L_1 and L_2 are Schiff base ligands of 4-aminoantipyrine and substituted salicylaldehydes, were synthesized and characterized using various spectroscopic techniques such as elemental analysis, UV–Vis, IR, and NMR. The single crystal X-ray structures for L_1, L_2, and their corresponding Cu(II) complexes assembled in a 1:2 metal to ligand ratio were analyzed for their various weak H-bonding and dimeric association. The structural analysis of compounds **1** and **2**, being the first crystal structures in this series, deserves special attention to help further the understanding in this area of structure–reactivity correlation studies. Further these compounds, composed of very similar chemical composition with a small difference in the substituent on the salicylaldehyde moiety, influenced through various weak inter- and intramolecular H-bonding and C–H$\cdots\pi$ interactions, rearrange the geometry around Cu(II) from a tetrahedrally distorted square planar geometry in $[Cu(L_1)_2]$ (**1**) to square planar in $[Cu(L_2)_2]$ (**2**). Steric strain imposed by the methyl substitution on the 4-aminoantipyrine moiety of the Schiff base ligand, causing this small change of the Cu(II) geometry, along with various weak interactions is analyzed in detail.

Keywords: Copper (II) complex; Crystal structure; Schiff base; Antipyrine

1. Introduction

Schiff bases of 4-aminoantipyrine and its complexes are known for their variety of applications in the area of catalysis [1,2], clinical applications [3], and pharmacology [4]. New kinds of chemo-therapeutic agents containing Schiff bases have gained significant attention among biochemists [1] and of those aminopyrines are commonly administered intravenously to detect liver disease [3] in clinical treatment. Hence a systematic understanding on the structure–reactivity correlation has warranted synthesis and characterization of a variety of Schiff base complexes containing different 2-hydroxy aromatic moieties such as furan-2-aldehyde, thiophene-2-aldehyde [4], and pyrrole-2-carboxaldehyde [5], etc. Thus there are a number of reports on compounds based on aminopyridine Schiff bases, though accounts of their crystal structures are limited. The salicylaldehyde based SAAP [6] and pyrrole based HPAP [5] Schiff base ligands and their Cu(II) [7] and lanthanum (Pr, Nd, Gd, Dy, Y, U) complexes [8,9] have been reported already. Although there are many compounds in the literature, our search on the CCDC shows no crystal structure has been reported so far and the structures of those entire complexes are elucidated only with spectroscopic evidence. With this in view, the present report accounts for the synthesis of two antipyrine Schiff base ligands L_1 and L_2 (Fig. 1) and their Cu(II) complexes $[Cu(L_1)_2]$ (**1**), and $[Cu(L_2)_2]$ (**2**), with a special impetus on their structural investigations. Further, the structural

* Corresponding authors. Tel.: +91 278 2567760; fax: +91 278 2566970 (P.S. Subramanian).
E-mail addresses: esuresh@csmcri.org (E. Suresh), siva140@yahoo.co.in (P.S. Subramanian).

0277-5387/$ - see front matter © 2006 Elsevier Ltd. All rights reserved.
doi:10.1016/j.poly.2006.09.004

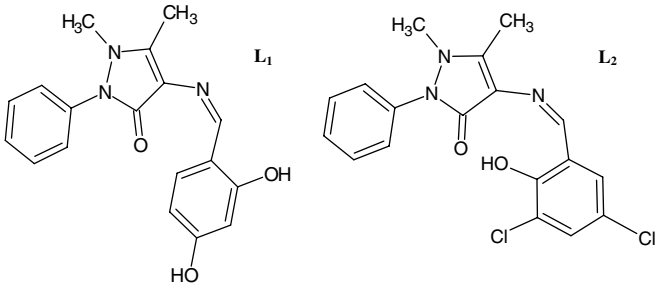

Fig. 1. Schiff base ligand system L_1 and L_2.

analysis in the present report explores that the weak interactions introduced by varying the substitution on the salicylaldehyde unit, modify the Cu(II) geometry from a tetrahedrally distorted square planar to a distorted square planar geometry.

2. Experimental

2.1. Materials

$Cu(CH_3COO)_2 \cdot H_2O$, 4-aminoantipyrine, 2,4-dihydroxybenzaldehyde, and 3,5-dichlorosalicylaldehydes were purchased from Aldrich & Co. All these chemicals were used as received without any further purification.

2.2. Synthesis

2.2.1. Preparation of the ligands: $L_1 \cdot MeOH$

A 1:1 equimolar methanolic solution of 4-aminoantipyrine (0.406 gm, 0.001 mol) and 2,4-dihydroxybenzaldehyde (0.276 gm, 0.001 mol) were mixed and gently heated for 2 h with constant stirring. The characteristic yellow precipitate obtained by Schiff base condensation was filtered out and kept for crystallization, dissolving in methanol. Fine yellow crystals obtained upon slow evaporation at room temperature were characterized, including single crystal X-ray diffraction. L_1: 4-{[(1*Z*)-(2,4-dihydroxyphenyl)methylene]-amino}-1,5-dimethyl-2-phenyl-1,2-dihydro-3*H*-pyrazol-3-one. NMR data (δ, *Methanol-d_4*): 13.55 (br s, –OH, 1H), 9.63 (s, CH=N, 1H), 7.56–7.20 (m, Ar phenyl, 5H), 6.40–6.31 (m, Ar, 3H), 3.14 (s, N–CH_3, 3H), 2.35 (s, C–CH_3, 3H). IR data (KBr, cm^{-1}): 3500–2900 (weak, br), 1615 (st, intense), 1586 (s, br). UV–Vis [CH_3CN, λ_{max}, nm, (ε, M^{-1}, cm^{-1})], 336 (3030), 422 (2840). ES [MSI] Calc for $C_{19}H_{21}N_3O_4$ (m/z+H^+) = 323.34. Found = 324.26. *Anal.* Calc. for $C_{19}H_{21}N_3O_4$: C, 64.21; H, 5.95; N, 11.82. Found: C, 63.86; H, 5.56; N, 12.25%.

2.2.2. Synthesis of L_2

4-{[(1*Z*)-(3,5-dichloro-2-hydroxyphenyl)methylene]amino}-1,5-dimethyl-2-phenyl-1,2-dihydro-3*H*-pyrazol-3-one. The above synthetic procedure was repeated for L_2 appropriately adapting 3,5-dichlorosalicylaldehyde in place of 2,4-dihydroxybenzaldehyde. NMR data (δ, $CDCl_3$): 14.3 (br s, OH, 1H), 9.75 (s, CH=N, 1H), 7.55-7.26 (m, Ar 7H), 3.23 (s, N-CH_3,3H), 2.45 (s, C–CH_3,3H). IR data (KBr, cm^{-1}) 3639–2593 (br), 1665 (sharp, st), 1589 (sharp, st). UV–Vis [CH_3CN, λ_{max}, nm, (ε, M^{-1}, cm^{-1})], 345 (3000), 380 (2800). ES [MSI] Calc for $C_{18}H_{15}Cl_2N_3O_2$ (m/z) = 375.05; Found = (m/z+H^+) = 376.25; (m/z+Na^+) = 398.24. *Anal.* Calc. for $C_{18}H_{15}Cl_2N_3O_2$; C, 57.46; H, 4.02; N, 11.17. Found: C, 57.5; H, 3.95; N, 11.0%.

2.2.3. Preparation of complexes $[Cu(L_1)_2]$ (**1**), and $[Cu(L_2)_2]$ (**2**)

The Schiff base ligand L_1 (0.071 gm, 0.002 mmol), dissolved in chloroform, was mixed with an ethanolic solution of $[Cu(CH_3COO)_2] \cdot H_2O$ (0.199 gm, 0.001 mmol) and allowed to stir continuously. The immediate color change from green to dark red indicates complexation. Upon slow evaporation at room temperature, the dark red crystals were obtained in 48 h. $[Cu(L_1)_2]$ (**1**): UV–Vis [CH_3CN, λ_{max}, nm, (ε, M^{-1}, cm^{-1})], 364 (1980), 509 (80). ES [MSI] Calc for $CuC_{36}H_{30}N_6O_6$ (m/z+H^+) = 708.18. Found = 708.30. *Anal.* Calc. for $CuC_{36}H_{30}N_6O_6$: C, 61.05; H, 4.55; N, 11.88. Found: C, 61.5; H, 4.48; N, 11.36%. $[Cu(L_2)_2]$ (**2**): The above procedure was repeated for **2** adapted for L_2 with a 1:2 $Cu(CH_3COO) \cdot H_2O$: L_2 ratio. UV–Vis [CH_3CN, λ_{max}, nm, (ε, M^{-1}, cm^{-1})], 359 (6970), 427 (1300), 531 (300). ES [MSI] Calc for $CuC_{36}H_{28}Cl_4N_6O_4$ (m/z+H^+) = 814.02. Found = 814.02. *Anal.* Calc. for $CuC_{36}H_{28}Cl_4N_6O_4$: C, 53.11; H, 3.46; N, 10.32. Found: C, 52.99; H, 3.97; N, 10.20%.

2.3. Physical measurements

Microanalysis of the complexes was done using a Perkin–Elmer PE 2400 series II CHNS/O elemental analyzer. IR spectra were recorded using KBr pellets (1% w/w) on a Perkin–Elmer Spectrum GX FT-IR spectrophotometer. Electronic spectra were recorded on a Schimadzu UV 3101PC spectrophotometer. Mass analyses were performed using electron spray ionization (ESI) technique on a Waters Q Tof-micro mass spectrometer. ^1H NMR spectra were recorded on a Bruker Avance DPX 200 FT-NMR spectrometer. Chemical shifts for proton resonances are reported in ppm (δ) relative to tetramethylesilane.

2.4. X-ray crystallography

A summary of the crystallographic data and details of data collection for L_1, L_2 and **1**, **2** are given in Table 1. Selected bond distances and bond angles for compounds **1** and **2** are given in Table 2. In each case, a crystal of suitable size was selected from the mother liquor and immersed in partone oil, then mounted on the tip of a glass fiber and cemented using epoxy resin. Intensity data for all three crystals were collected using Mo Kα (λ = 0.71073 Å) radiation on a Bruker SMART APEX diffractometer equipped with a CCD area detector. The data integration and reduction were processed with SAINT [10] software. An empirical

Table 1
Summary of crystallographic data for the compounds

Code	L_1	L_2	1	2
Chemical formula	$C_{19}H_{21}N_3O_4$	$C_{18}H_{15}Cl_2N_3O_2$	$C_{36}H_{32}Cu_1N_6O_6$	$C_{18}H_{14}Cl_2Cu_{0.50}N_3O_2$
Formula weight	355.39	376.23	708.22	406.99
a (Å)	13.9443(16)	7.0141(8)	10.2073(16)	23.197(2)
b (Å)	6.8950(8)	8.0449(9)	12.1721(19)	6.7034(6)
c (Å)	19.390(2)	30.487(3)	13.776(2)	22.443(2)
α (°)	90.0	90	74.189(3)	90
β (°)	109.953(2)	90.972(2)	74.273(3)	90.918(3)
γ (°)	90	90	80.569(3)	90
Z	4	4	2	8
V (Å^3)	1752.4(3)	1720.1(3)	1577.7(4)	3489.4(6)
Crystal system	monoclinic	monoclinic	triclinic	monoclinic
Space group	$P2_1/c$	$P2_1/n$	$P\bar{1}$	$C2/c$
Radiation used, λ (Å)	0.71073	0.71073	0.71073	0.71073
$\rho_{calc.}$ (g cm^{-3})	1.347	1.453	1.491	1.549
Absolute coefficient, μ (mm^{-1})	0.096	0.394	0.751	0.983
Temperature (K)	100	293	293	293
R_1 on $[(F_o^2)]$[a]	0.0534	0.0482	0.0621	0.0382
wR_2 on (F_o^2)[b]	0.1285	0.1237	0.1526	0.0954

[a] $R = \sum \|F_o| - |F_c\| / \sum |F_o|$.

[b] $R_w = [Sw(F_o^2 - F_c^2)^2]/S[w(F_o^2)^2]^{1/2}$; $w = 1/\sigma(F_o)^2$.

Table 2
Selected bond distances (Å) and angles (°) for complexes **1** and **2** with estimated standard deviations in the parenthesis

	1	2
Bond length (Å)		
Cu(1)–O(3)	1.887(3)	
Cu(1)–O(2)		1.8878(14)
Cu(1)–O(2)#1		1.8878(14)
Cu(1)–O(6)	1.924(3)	
Cu(1)–N(6)	1.953(3)	
Cu(1)–N(3)	1.967(3)	1.9567(17)
Cu(1)–N(3)#1		1.9567(17)
Bond angle (°)		
O(3)–Cu(1)–O(6)	91.78(12)	
O(3)–Cu(1)–N(6)	145.30(13)	
O(6)–Cu(1)–N(6)	94.07(13)	
O(3)–Cu(1)–N(3)	95.95(13)	
O(6)–Cu(1)–N(3)	143.74(13)	
N(6)–Cu(1)–N(3)	99.23(13)	
O(2)#1–Cu(1)–O(2)		154.31(9)
O(2)#1–Cu(1)–N(3)#1		90.75(6)
O(2)–Cu(1)–N(3)#1		93.63(6)
O(2)#1–Cu(1)–N(3)		93.63(6)
O(2)–Cu(1)–N(3)		90.75(6)
N(3)#1–Cu(1)–N(3)		160.18(10)

absorption correction was applied to the collected reflections using SADABS [11]. The structures were solved by direct methods using SHELXTL [11b] and were refined on F^2 by the full-matrix least-squares technique using the SHELXL-97 [12] package. Graphics are generated using ORTEP. Packing and H-bonding diagrams are generated by PLATON [13] and MERCURY [116]. In all the four compounds, non-hydrogen atoms were refined anisotropically until convergence was reached and hydrogen atoms attached to all carbon atoms were geometrically fixed using the program SHELXTL.

3. Results and discussion

3.1. Spectral investigation

The Schiff base ligands L_1 and L_2 are yellow in color and are soluble in almost all organic solvents, such as methanol, acetonitrile, chloroform, acetone, DMF and DMSO, and the corresponding metal complexes $[Cu(L_1)_2]$ (**1**) and $[Cu(L_2)_2]$ (**2**) obtained with a 1:2 metal ligand ratio are found to be dark red in color. The electronic spectra for both these ligands behave very similarly and show two characteristic bands at 336–360 nm and 420 nm representing intra ligand charge transfer transitions. The corresponding metal complexes **1** and **2** exhibit a characteristic d-d band at 500–530 nm with a broad spectral feature. While the position of λ_{max} is attributable to the square planar geometry, the broadness of the spectral pattern can be attributed to the degree of distortion in the geometry. The three characteristic IR signals for L_1 and L_2, corresponding to (i) OH; (ii) C=O, C=N; (iii) phenolate oxygen C···O, were analyzed. The broad IR signal centered at 3430 cm^{-1} obtained for both the free ligands L_1 and L_2 can be ascribed to the OH functional groups. The compounds **1** and **2** show sharp and intense peaks in the range of 1572–1589 cm^{-1} and 1616–1665 cm^{-1} which can be attributed to $\nu_{CH=N}$ and $\nu_{C=O}$ stretching modes respectively. The characteristic peak at 9.6–9.75 δ in the ^{1}H NMR spectrum further confirms the azomethine CH=N condensation. The disappearance of the OH peak and the significant shift in the $\nu_{C=N}$ stretching frequency in **1** and **2**, with respect to the corresponding free ligands, indicate the complexation with the Cu(II) center. The shift in the azomethine peak by 10–15 cm^{-1} in the IR spectra indicates its involvement in coordination. The IR signal observed at

1616–1665 cm^{-1}, representing the C=O group attached to the antiypyrine five-membered ring remains unchanged in compounds **1** and **2** with respect to the free ligands, symbolizing that it is not involved in the coordination.

3.2. Crystal structure and molecular association

3.2.1. Structure of L_1

The Schiff base ligand L_1 crystallizes in the monoclinic space group $P2_1/c$, along with methanol as a solvent of crystallization. Fig. 2a–c represents the ORTEP diagram for L_1, its dimeric association and the intermolecular C–H···N interaction through molecular pairs along the *c*-axis, respectively. The *meta*-dihydroxy substituted salicylyl phenyl ring C11–C16 is almost in the same plane (mean plane deviation 12.89°), while the phenyl ring C1–C6 of the antipyrine moiety is tilted by 49.67° with respect to the central five-membered ring. The mode of molecular packing influenced through the mode of H-bonding is dictated by variation in the substitutions on the salicyl phenyl ring.

As depicted in Fig. 2b, the molecules are oriented in such a way that the C18 methyl group of the antipyrine ring is aligned towards the azomethine N3, making strong intermolecular C–H···N interactions forming molecular pairs along the *c*-axis [C(18)–H(18A)···N(3); H(18A)···N(3) = 2.58 Å C(18)···N(3) = 3.536(2) Å, ∠C(18)–H(18A)···N(3) = 171°, symmetry code: $1-x, -1/2+y, 1/2-z$]. H18C from the same methyl group is involved in an intermolecular C–H···O interaction with the exocyclic ketonic oxygen of the antipyrine ring along the *b*-axis [C(18)–H(18C)···O(1); H(18C)···O(1) = 2.41 Å, C(18)···O(1) = 3.358(2) Å, ∠C(18)–H(18C)···O(1) = 167° symmetry code: $x, -1+y, z$] which is well within the range in the review articles reported by Steiner [15a] and Nangia [15b]. In addition to the C–H···N interaction, the lattice methanolic OH acts as both donor and acceptor through O–H···O hydrogen bonding with the molecular pairs (Fig. 2b) of the L_1 moiety from either side creating a layered hydrogen bonded motif. The O–H···O hydrogen bonding parameters, with the symmetry code, between the lattice methanol with ketonic oxygen O1 of the antipyrine ring and the phenolic hydrogen H2A of the ligand moiety are as follows: O(4)–H(4A)···O(1); H(4A)···O(1) = 1.86 Å; O(4)···O(1) = 2.671(2) Å, ∠O(4)–H(4A)···O = 171°, symmetry code: $1-x, -1/2+y, 3/2-z$ and O(2)–H(2A)···O(4):H(2A)···O(4) = 1.85 Å, O(2)···O(4) = 2.665(2) Å, ∠O(2)–H(2A)···O(4) = 171°, symmetry code: $x, 5/2-y, -1/2+z$. In addition to this intermolecular hydrogen bonding, intramolecular O–H···N and C–H···O interactions also exist for the stabilization of the ligand moiety, incorporating the methanol molecule in the crystal lattice (Fig. 2c).

3.2.2. Structure of L_2

Ligand L_2 crystallizes in monoclinic space group $P2_1/n$ with four molecules in the unit cell. Fig. 3a and b represents the ORTEP diagram and their dimeric association of L_2. In L_2, the *ortho* and *para* positions of the phenyl ring, with respect to the OH group, are substituted by Cl1 and Cl2 respectively. The dichloro substituted "sal" phenyl ring (C11–C16) is in the same plane, while the phenyl ring C1–C6 of the antipyrine moiety is tilted by 36.64° with respect to the central five-membered ring. The tilt of the phenyl group (C1–C6) with respect to central five-membered ring can be attributed to various molecular interactions involved in the packing pattern.

The molecules are packed along the *ac*-plane with a slight offset in adjacent layers to make an effective dimeric

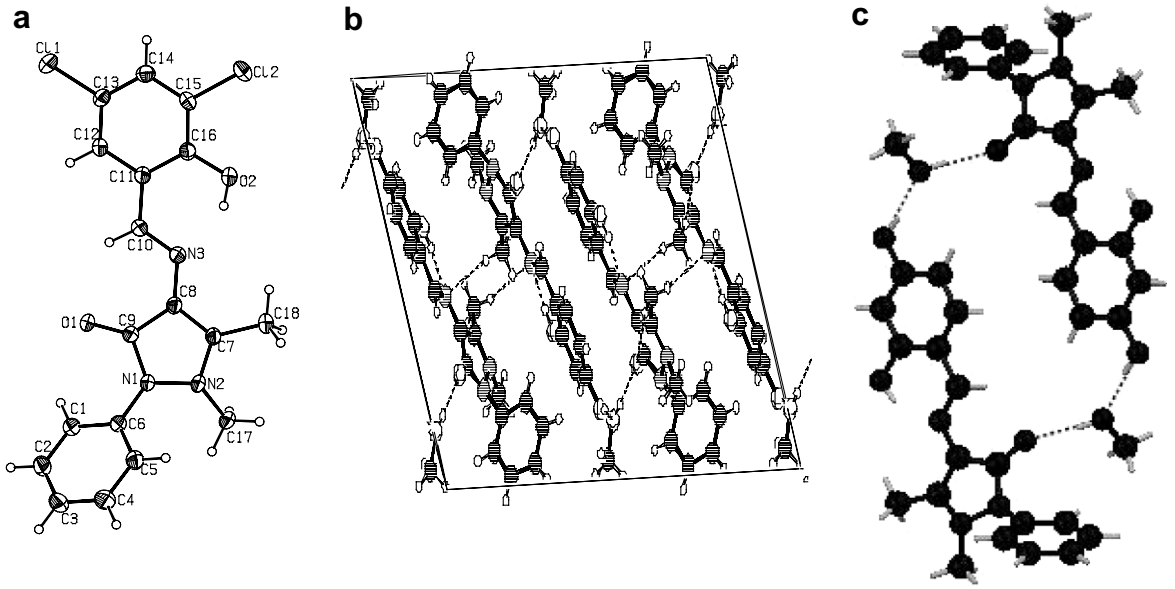

Fig. 2. (a) ORTEP diagram with the atom numbering for L_1, (b) intermolecular CH···N interaction mediated molecular pairs and (c) dimeric association through methanol.

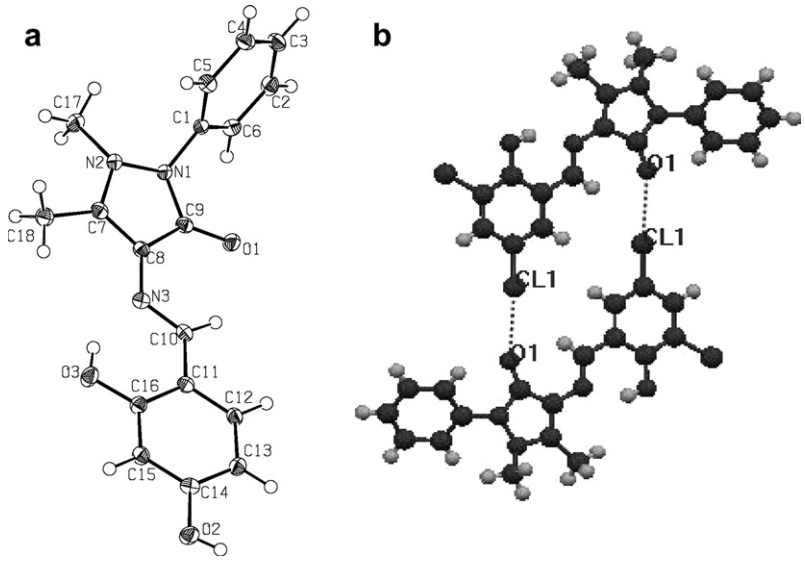

Fig. 3. (a) ORTEP diagram with the atom numbering for L_2 and (b) dimeric association of L_2.

association via a C=O···Cl interaction. The close up view of the dimeric association via the C=O···Cl interaction between a centro-symmetric pair is shown in Fig. 3b. Thus, Cl1 attached to the "sal" phenyl ring makes contact with the exocyclic ketonic oxygen O1 of the five-membered antipyrine ring with an O···Cl distance of 3.010 Å and angle ∠C=O···Cl of 158.12°, which is well within the range reported earlier [15c]. The observed O···Cl distance (3.010 Å) is shorter than the sum of the Van der Waals radii for Cl and O (3.2 Å) and this short contact is due to the partial positive and negative charge residing on Cl1 and O1 respectively. Further, the O···Cl short contacts observed in pentachloronitrobenzene by Tanaka et al. [15d] and 2-chloro-4,6-dinitrophenol by Andersen et al. [15e] also support a similar mode of interaction with partial negative and positive charges between the O and Cl atoms at a distance 3.01 Å and 3.054 Å, respectively. Intramolecular O–H···N H-bonding between the phenolic hydrogen H2 and N3 (O(2)–H(2)···N(3):H(2)···N(3) = 1.87 Å; O(2)···N(3) = 2.597(2) Å; ∠O(2)–H(2)···N(3) = 148°) and a C–H···O interaction (C(10)–H(10)···O(1):H(10)···O(1) = 2.28 Å; C(10)···O(1) = 2.972(3) Å and C(10)–H(10)···O(1) = 130°) between H10 and the exocyclic ketonic oxygen O1 of the five-membered ring are also observed, and these intramolecular H-bonding interactions have an effect on the conformation of the molecule, including the tilt of the phenyl ring with respect to the five-membered ring.

3.2.3. Structure of $[Cu(L_1)_2]$ (1)

An ORTEP view of the neutral Cu(II) complex, **1** with the atom numbering scheme is shown in Fig. 4. The metal center possesses a tetrahedrally distorted square planar geometry with N2O2 donor atoms coordinating from two different Schiff base ligands L_1. Even though the ligand is tridentate in nature, it binds the Cu(II) ion, in a bidentate fashion through the deprotonated phenolic oxygen of the phenyl ring and nitrogen of the azomethine group, leaving

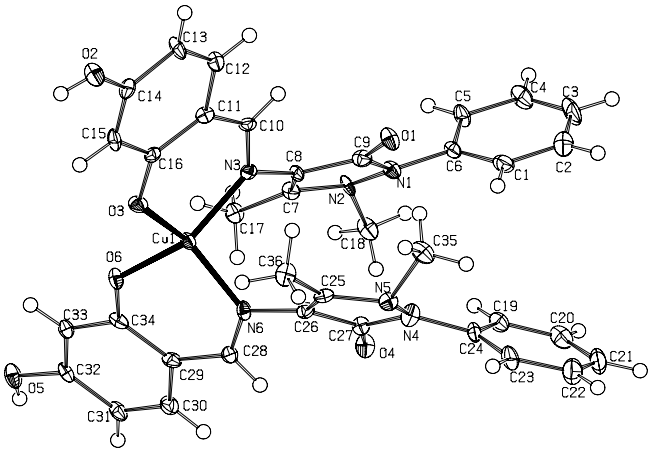

Fig. 4. ORTEP diagram of *1* with the atom numbering scheme.

the antipyrine exocyclic ketonic oxygen O4 and O1 free. The steric strain imposed by the methyl substitution on the antipyrine moiety restricts the ligand towards bidentate coordination from its tridentate nature. The Cu–N distances (Cu1–N3 = 1.967(3) Å; Cu1–N6 = 1.953(3) Å) and Cu–O distances (Cu1–O3 = 1.887(3) Å; Cu1–O6 = 1.924(3) Å) are well within the range reported for related Schiff base complexes of Cu(salen) [16,17]. The *cis* angles subtended by the six-membered chelate ring with Cu(II) from each ligand [O3–Cu1–N3 = 95.95(13)°, O6–Cu1–N6 = 94.07(13)°, N6–Cu1–N3 = 99.23(13)°, O3–Cu1–O6 = 91.78(12)°] deviate only marginally from the ideal square planar value. However, the trans angles [N6–Cu1–O3 = 145.30(13)° and O6–Cu1–N3 = 143.74(13)°] at the Cu(II) center deviate significantly from an ideal square planar geometry, indicating a tetrahedral bias to the Cu(II) coordination. This may be due to the steric constraints imposed by the methyl groups attached to the five-membered antipyrine ring towards the right approach of

the ligand moiety for metal coordination. This is further strengthened by the mean plane involving the "sal" units from different ligands, which are twisted relative to each other by approximately 58.09° and make angles of 28.86° (C11–C16 and O3) and 37.89° (C29–C34 and O6) with respect to the N2O2 mean plane. The N and O atoms show considerable deviation from the mean plane involving N2O2; *trans* N and O from a different ligand moiety (N3 and O6) are displaced in the downward direction (−0.540 Å and −0.625 Å) while N6 and O3 are in the opposite direction (0.494 Å and 0.540 Å) with Cu(II) contained well within the coordination plane (0.015 Å). It is pertinent to note that such distortions in the Cu(II) geometry of blue copper proteins [18–20] and Cu(salen) [21,22] complexes with tetrahedrally distorted square planar geometry are reported to deserve importance in view of catalytic activity.

The packing diagram viewed down the *a*-axis with various H-bonding interactions in **1** is depicted in Fig. 5. The molecules are aligned as layers along the *b*-axis by strong intermolecular O–H···O interactions, between adjacent molecules via the phenolic hydrogen H5 (from O5) of each coordinated ligand moiety with the ketonic oxygen O1 of the five-membered antipyrine moiety. These hydrogen bonded layers are further cross linked along the *c*-axis generating the bilayer by another intermolecular O–H···O H-bonding between the phenolic hydrogen H2 of the second ligand with the coordinated "sal" oxygen O2 [O(2)–H(2)···O(6):H(2)···O(6) = 1.97 Å, O(2)···O(6) = 2.701(4) Å, ∠O(2)–H(2)···O(6) = 147°]. Intermolecular C–H···O interactions between the bilayers creates a two dimensional H-bonded network in the *bc*-plane [C(17)–H(17A)···O(3):H(17A)···O(3) = 2.51 Å, C(17)···O(3) = 3.323(5) Å, ∠C(17)–H(17A)···O(3) = 142° and C(22)–H(22)···O(2):H(22)···O(2) = 2.43 Å, C(22)···O(2) = 3.340(6) Å,∠C(22)–H(22)···O(2) = 167°]. In addition to the above mentioned intermolecular H-bonding, intramolecular C–H···O H-bonding also exist between the methyl hydrogens H18A and H35A from different ligands with the ketonic oxygens O4 and O1 respectively (C(18)–H(18A)···O(4):H(18A)···O(4) = 2.49 Å; C18···O(4) = 3.364(6), ∠C(18)–H(18A)···O(4) = 151° and C(35)–H(35A)···O(1):H(35A)···O(1) = 2.31 Å, C(35)···O(1) = 3.242(6) Å and ∠C(35)–H(35A)···O(1) = 162°). Thus, the ketonic oxygen O1 and O4 from the two different ligand moieties may be orienting the preferential hydrogen bonding mode rather than coordination with the metal center to impose a tetrahedrally distorted square pyramidal geometry around the Cu(II) center.

3.2.4. Structure of $[Cu(L_2)_2]$ (2)

Compound **2** crystallizes in the centrosymmetric space group $C_{2/c}$ with Cu(II) sitting on a twofold axis. An ORTEP view of the neutral Cu(II) complex with the atom numbering scheme is shown in Fig. 6. The metal center possesses a distorted square planar geometry with N2O2 donor atoms coordinating from two different Schiff base ligands. The Cu(II) ion occupies a special position and coordinates with two symmetry related ligand moieties in a bidentate fashion through the deprotonated phenolic oxygen and nitrogen of the azomethine group, leaving the antipyrine exocyclic ketonic oxygen free. The Cu–N distance (Cu1–N3 = 1.9567(17) Å) and Cu–O distance (Cu1–O2 = 1.8878(14) Å) are well within the range reported for related Schiff base complexes [16,17]. The *cis* angles subtended by the six-membered chelate ring with Cu(II) from each ligand [O2–Cu1–N3 = 90.75(6)°, O(2)a–Cu(1)–N(3) = 93.63(6)°] are within the close range of an ideal square planar value, while the *trans* angles [O(2)a–Cu(1)–O(2) = 154.31(9)° and N(3)a–Cu(1)–N(3) = 160.18(10)°] at the Cu(II) center deviate from square planar geometry, indicating a distorted square planar geometry for the Cu(II) coordination. This can be attributed to the six-membered metal-chelate ring formation by the ligand moiety around Cu(II) and the ligand steric constraints imposed by the methyl groups attached to the five-membered antipyrine ring towards the closer approach for metal coordination. The mean

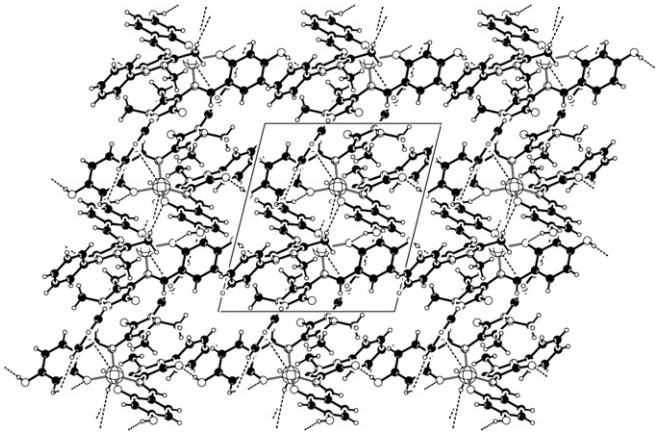

Fig. 5. Packing diagram of **1** viewed down the *a*-axis with various H-bonding interactions.

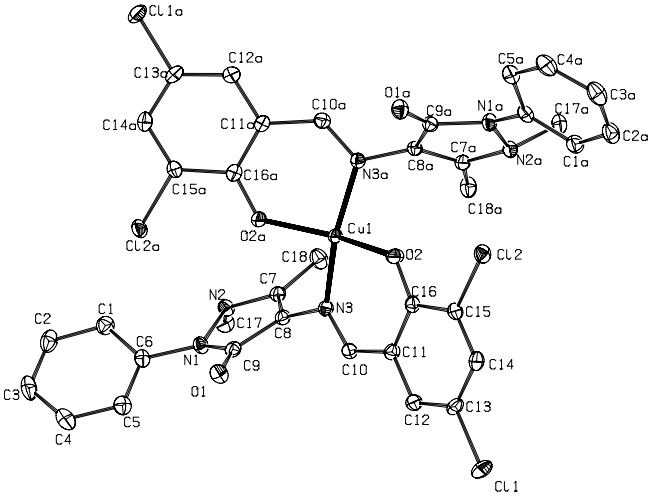

Fig. 6. ORTEP diagram of **2** with the atom numbering scheme. (Hydrogen atoms are omitted for clarity.)

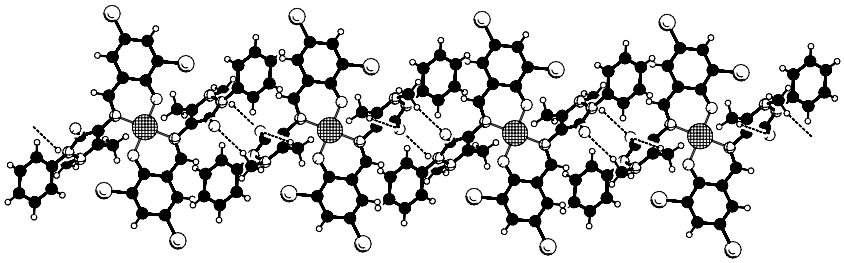

Fig. 7. Packing diagram of **2** viewed down the *b*-axis showing the hydrogen bonding interactions.

plane involving the "sal" units of symmetry related ligands are twisted relative to each other by 34.43° and make a 17.15° angle (angle of C11–C16 and O2) with respect to the N2O2 mean plane, which is comparatively less in **2** indicating much less distortion from the square planar geometry. The Cu(II) atom is contained well in the square base, the *trans* oxygens and *trans* nitrogens coordinated to it from the twofold related ligands are displaced by 0.729° and 1.789° respectively in opposite directions.

A packing diagram of compound **2** viewed down the *b*-axis with hydrogen bonding interactions is shown in Fig. 7. As depicted in the packing, the molecules are arranged in layers along the *c*-axis. The aligned adjacent molecules within the layers are bridged via intermolecular C–H···O hydrogen bonding between the methyl hydrogens H17C and H18C of the five-membered antipyrine ring with the exocyclic ketonic oxygen O1 from either side of the symmetry allied ligand moiety. Details pertinent to the hydrogen bonding interactions and symmetry code are: C(17)–H(17C)···O(1):H(17C)···O(1) = 2.38 Å; C(17)···O(1) = 3.303(3) Å; ∠C(17)–H(17C)···O(1) = 160°, symmetry code: $-x$, $1-y$, $-z$ and C(18)–H(18C)···O(1):H(18C)···O(1) = 2.57 Å; C(18)···O(1) = 3.502(3); ∠C(18)–H(18C)···O(1) = 163°, symmetry code; x, $1+y$, z. The layers along the *c*-axis are also involved in weak C–H···π interactions [23] between the antipyrine phenyl ring and azomethane hydrogen H10, showing the effective closer approach and orientation of the neighboring molecules. Pertinent C–H···π interactions with the symmetry code are C10–H10···Cg1:H10···Cg1 = 2.94 Å, C10···Cg1 = 3.609(2) Å and ∠C10–H10···Cg1 = 130°, symmetry code = $-x$, $1-y$, $-z$, where Cg1 is the centroid of the phenyl ring (C1–C6). In the crystal structures of 5-dimethylnaphthalene [23b] and Resorcinol [23c] the observed CH···π distances range from 2.87 Å to 2.99 Å and 2.77 Å to 2.92 Å which are comparable with the present report for a weak C–H···π contact.

4. Conclusion

In conclusion, we have synthesized two important antipyrine Schiff base ligands and their Cu(II) complexes. The single crystal X-ray structures of **1** and **2**, being the first in the series of this type of compound, illustrate that the mode of weak H-bonding interactions and steric effect imposed by the methyl group has a profound influence on the Cu(II) geometry in **1** and **2**, rearranging from tetrahedrally distorted square planar geometry into distorted square planar.

Acknowledgements

The authors greatly acknowledge Dr. P.K. Ghosh Director of the Central Salt and Marine Chemicals Research Institute for his keen interest and encouragements. The authors P.S. and M.S. acknowledge DST, New Delhi, for the financial support

Appendix A. Supplementary material

CCDC 614053, 614054, 614055 and 614056 contain the supplementary crystallographic data for this paper. These data can be obtained free of charge via http://www.ccdc.cam.ac.uk/conts/retrieving.html, or from the Cambridge Crystallographic Data Centre, 12 Union Road, Cambridge CB2 1EZ, UK; fax: (+44) 1223-336-033; or e-mail: deposit @ccdc.cam.ac.uk. Supplementary data associated with this article can be found, in the online version, at doi:10.1016/j.poly.2006.09.004.

References

[1] K. Bernardo, S. Leppard, A. Robert, G. Commenges, F. Dehan, B. Meunier, Inorg. Chem. 35 (1996) 387.
[2] T. Punniyamurthy, S.J.S. Kalra, J. Iqbal, Tetrahedron Lett. 36 (1995) 8497.
[3] D. Chiaramonte, J.M. Steiner, J.D. Broussard, K. Baer, S. Gumminger, E.M. Moeller, D.A. Williams, R. Shumway, Can. J. Vet. Res. 67 (2003) 183.
[4] (a) A.M. Farghaly, A. Hozza, Pharmazie 35 (1980) 596;
(b) T. Hitoshi, N. Tamao, A. Hideyuki, F. Manabu, M. Takayuki, Polyhedron 16 (1997) 3787.
[5] Kamal.Z. Ismail, Transition Met. Chem. 25 (2000) 522.
[6] A. El-Dissouky, A.K. Shehata, G. El-Mahadey, Polyhedron 16 (1997) 1247.
[7] N. Raman, A. Kulandaisamy, C. Thangaraja, Transition Met. Chem. 29 (2004) 129.
[8] G. Shankar, R.R. Premkumar, S.K. Ramalingam, Polyhedron 5 (1986) 991.
[9] T. Radhakrishnana, P.T. Joseph, C.P. Prabhakaran, J. Inorg. Nucl. Chem. 38 (1976) 2212.
[10] G.M. Sheldrick, SAINT, 5.1 ed., Siemens Industrial Automation Inc., Madison, WI, 1995.
[11] (a) SADABS, Empirical Absorption Correction Program, University of Göttingen, Göttingen, Germany, 1997;
(b) G.M. Sheldrick, SHELXTL Reference Manual: Version 5.1, Bruker AXS, Madison, WI, 1997.

[12] G.M. Sheldrick, SHELXL-97: Program for Crystal Structure Refinement, University of Göttingen, Göttingen, Germany, 1997.
[13] A.L. Spek, PLATON-97, University of Utrecht, Utrecht, The Netherlands, 1997.
[14] Mercury 1.3 Supplied with Cambridge Structural Database; CCDC: Cambridge, UK, 2003–2004.
[15] (a) T. Steiner, Angew. Chem., Int. Ed. 41 (2002) 48;
(b) A. Nangia, Cryst. Eng. Commun. 4 (17) (2002) 93;
(c) P.N. Moorthy, P. Venkatakrishnan, P. Mal, S. Dixit, P. Venugopalan, Cryst. Growth Des. 3 (2003) 581;
(d) I. Tanaka, F. Iwasaki, A. Aihara, Acta Crystallogr., Sect. B 30 (1974) 1546;
(e) E.K. Andersen, I.G.K. Andersen, Acta Crystallogr., Sect. B 31 (1975) 387.
[16] M.M. Bhadbhade, D. Srinivas, Inorg. Chem. 32 (1993) 6122.
[17] P.S. Subramanian, E. Suresh, P. Dastidar, Polyhedron 23 (2004) 2515.
[18] (a) A. Messerschmidt, Struct. Bond. 90 (1998) 37;
(b) E.I. Solomon, K.W. Penfield, D.E. Wilcox, Struct. Bond. 53 (1983) 1.
[19] A. Messerschmidt, Adv. Inorg. Chem. 40 (1994) 121.
[20] A.G. Sykes, Adv. Inorg. Chem. 36 (1991) 377.
[21] C.R. Jacob, S.P. Varkey, P. Ratnasamy, Micropor. Mesopor. Mater. 22 (1998) 465.
[22] C.R. Jacob, S.P. Varkey, P. Ratnasamy, Appl. Catal. A 168 (1998) 353.
[23] (a) Y. Umezawua, S.T. Sudoyama, K. Honda, J. Uzawa, M. Nishio, Bull. Chem. Soc. Jpn. 71 (1998) 1207;
(b) A.C. Hazell, R.G. Hazell, L. Norskov-Lauristein, C.E. Briant, D.W. Jones, Acta Crystallogr., Sect. C 42C (1986) 690;
(c) G.E. Bacon, R.J. Jude, Z. Kristallogr. 138 (1973) 19.